Title

A Direct Integral Method for the Analysis of Borehole Fluid Conductivity Logs to Determine Fracture Inflow Parameters

Authors

Tsang, C.F.
Hale, F.

Publication Date

1989-03-01

LBL-27930

Lawrence Berkeley Laboratory

UNIVERSITY OF CALIFORNIA

EARTH SCIENCES DIVISION

Presented at the National Water Well Association Conference
on New Techniques for Quantifying the Physical and
Chemical Properties of Heterogeneous Aquifers,
Dallas, TX, March 20–23, 1989, and
to be published in the Proceedings

A Direct Integral Method for the Analysis of Borehole Fluid Conductivity Logs to Determine Fracture Inflow Parameters

C.-F. Tsang and F. Hale

March 1989

Prepared for the U.S. Department of Energy under Contract Number DE-AC03-76SF00098.

DISCLAIMER

LBL-27930

A Direct Integral Method for the Analysis of Borehole Fluid Conductivity Logs to Determine Fracture Inflow Parameters

Chin-Fu Tsang and Frank Hale

Earth Sciences Division
Lawrence Berkeley Laboratory
1 Cyclotron Road
Berkeley, California 94720

March 1989

This work was supported by the Director, Office of Energy Research, Office of Basic Energy Sciences, Engineering and Geosciences Division, and the Director, Office of Civilian Radioactive Waste Management, Repository Technology Division (DOE/CH), of the U.S. Department of Energy under Contract No. DE-AC03-76SF00098.

A Direct Integral Method for the Analysis of Borehole Fluid Conductivity Logs to Determine Fracture Inflow Parameters

Chin-Fu Tsang and Frank Hale

Earth Sciences Division
Lawrence Berkeley Laboratory
One Cyclotron Road
Berkeley, CA 94720

Abstract

It is of much current interest to determine the flow characteristics of fractures intersecting a wellbore in order to provide data in the estimation of the hydrologic behavior of fractured rocks. Often inflow from these fractures into the wellbore is at very low rates. In addition very often one finds that only a few percent of the fractures identified by core inspection and geophysical logging are water-conducting fractures, the rest being closed, clogged or isolated from the water flow system. A new procedure is proposed and a corresponding method of analysis developed to locate water-conducting fractures and obtain fracture inflow rates by means of a time sequence of electric conductivity logs of the borehole fluid. The physical basis of the analysis method is discussed. The procedure is applied to a synthetic set of data, which shows initiation and growth of four conductivity peaks in a 900-m section of a 1690-m borehole, corresponding to water-conducting fractures intersecting the borehole. We are able to match all four peaks and determine the flow rates as well as the salinity of the water from these fractures.

Introduction

In the study of the hydrology of fractured rocks, it is important to know the fracture properties. Surface observations may be useful, but the more relevant observations are those made at the depths of interest. Such measurements are mainly carried out through boreholes or underground openings. In the case of boreholes various methods of studying fracture properties have been used. For example, a downhole televiewer can be used to map the fracture traces on the borehole walls and determine their density and orientations. However, it is well known that often these traces do not correspond to locations of water-conducting fractures. Hence, there is a need to (1) identify the location and (2) measure directly the hydraulic or flow properties of an identified water-conducting fracture or group of fractures intersected by the borehole.

Constant-pressure, constant-flow or pulse tests have been applied to packed intervals along a wellbore. Since many of the fractured rocks of interest are of low permeability, the flow from a packed interval can be very slow. This has necessitated the development of low-flow measurement tools and the use of long-term measurements involving many packed intervals tested one at a time. Packed-off test intervals are usually larger than individual water-conducting zones, thus leading to an uncertainty in the location of a water-bearing fracture. An alternative method is the measurement of inflow along the borehole from fractures without the use of packers, with the well flowing at a moderate rate. Borehole flowmeters (see e.g., Hufschmied, 1983; Omega, 1987; Bean, 1971) can in principle yield the inflow rate from individual inflow zones. Such a flow- meter log is often strongly affected by wellbore radius variations. Thus, a caliper log has to be run to calibrate the results. Also, there is a low flow rate limit below which the conventional flowmeter log is no longer useful.

A more recent method using a heat pulse for measuring low velocities in boreholes (Paillet et al., 1987, Hess, 1985) can measure much lower flow velocities than conventional flowmeters, especially when an inflatable packer is used to direct flow through the heat pulse flowmeter.

The present paper describes a new method involving the use of a time sequence of electric conductivity logs of borehole fluid without the use of packers. The following section describes the logging procedure and the analysis method used. Next, analytic considerations are discussed to show the functional dependence and expected results for the short and long time limits. Then the numerical method used in the data analysis is introduced and applied to a set of synthetic data based on field data from the Leuggern borehole in Switzerland.

Fluid Conductivity Logging Procedure

Consider the uncased section of a wellbore that intersects a number of flowing fractures. In general, the flowing fractures contain fluids with different chemical compositions and ion content, and hence different electric conductivities. The relationship between ion concentration and fluid electric conductivity is reviewed, for example, by Shedlovsky and Shedlovsky (1971), who give graphs and tables relating these two quantities. Hale and Tsang (1988) made a sample fit for the case of NaCl solution at low concentrations and obtained

$$\sigma = 0.187C - 0.004C^2 \tag{1}$$

where σ is the fluid electric conductivity in S/m and C is concentration of NaCl in kg/m^3. The formula is valid at a temperature of 20°C, and for values of C up to about 6 kg/m^3 and values of σ up to 1.1 S/m (or 11000 μS/cm). The quadratic term can be dropped if one is interested only in values of C up to about 4 kg/m^3 and σ up to 0.8 S/m (or 8000 μS/cm). In this case we have a convenient linear relationship between σ and C:

$$\sigma(\mu S/cm) = \alpha C(kg/m^3) \tag{2}$$

where $\alpha = 1870\ (\mu S/cm) \cdot (m^3/kg)$ and the units were chosen because in the field data we analyzed σ is given in μS/cm .

Suppose the wellbore is first washed out with de-ionized water by passing a tube to the well bottom. There will be some residual ion content and associated electric conductivity (e.g. about 60 μS/cm, corresponding to a residual salinity concentration of 0.03 kg/m^3). Now let us produce from the wellbore at a flow rate Q. For three fractures we have a situation shown schematically in Figure 1. Note that the flow rates at different parts of the wellbore are different, being equal to the sum of all upstream inflow rates. At each fracture inflow point, the parameters characterizing the flow are t_{oi}, the time when the fracture fluid emerges at the wellbore; x_i, the location of the inflow point; q_i, the volumetric inflow rate; and q_iC_{oi}, the solute mass inflow rate, where C_{oi} is the concentration of ionic solutes in the fracture fluid. Here we have assumed that generally t_{oi} can be different for different fracture inflow points. This could be due to different initial hydraulic heads in these fractures or the specific borehole development and pressure history, with the result that the de-ionized water enters the fractures during borehole-washing out. Thus when the wellbore is produced at flow rate Q, the de-ionized water from the fractures first returns to the borehole, delaying the arrival of in-situ fracture water. These arrival times can be different for the different fractures.

Figures 2-5 display schematically salinity distribution inferred from fluid electric conductivity distribution in the wellbore for a series of times. Figure 2 shows the curves for early values of time. In this paper we assume that the wellbore cross section is small compared with its length, so that salinity or chemical concentration is uniform at each cross section. If there is no overall upward flow in the wellbore and density effects can be neglected, one expects the salinity curves at each inflow point to be symmetrical about the inflow point (see formula in the next section). When the well is pumped at a given flow rate, a skewing of the curves is expected due to the upward flow in the wellbore, which is larger near the well top than near the well bottom.

Figures 3-5 show three possible sets of salinity curves for large time periods, all assuming very small borehole diffusivity. Figure 3 shows one possible set of results. At large times, the saturation salinity is given by

$$C_{max,i} = \frac{wC_o + q_iC_i}{w + \sum_{n=1}^{i} q_n} \tag{3}$$

where q_i is the inflow rate, with i = 1 corresponding to the deepest inflow point of the flow survey (i.e., most upstream), and w is the borehole flow rate from below the surveyed section, and C_o is the initial salinity of wellbore water. If the salinity curves from two inflow points i and i + 1 overlap, then $C_{max,i}$ is still given by (1), but $C_{max,i+1}$ is given by

$$C_{max,i+1} = \frac{wC_o + q_iC_i + q_{i+1}\, C_{i+1}}{w + \sum_{n=1}^{i+1} q_n} \tag{4}$$

There is a step-jump at the location of the (i+1)-th inflow point when the salinity curve from i-th inflow reaches the (i+1)-th location. This is demonstrated in Figure 3 for three inflow points, with second and third inflow salinity curves interfering with each other.

At the limit of very large time periods, the expected salinity curves are shown in Figure 4. Here the step structure is prominent, with the C_{max} value between the i-th and (i+1)-th inflow points given by

$$C_{max,i} = \frac{wC_o + \sum_{n=1}^{i} q_n C_n}{w + \sum_{n=1}^{i} q_n} \tag{5}$$

With diffusion, the step structure will be smeared out. Note that the results, equations (3), (4) and (5), are independent of variations of wellbore radius.

Figure 5 shows a sequence of curves from early to later times. In this figure, the effect of having one of the three inflows starting much earlier than the other two is shown.

Thus, the procedure for fluid conductivity logging is as follows. After the wellbore fluid is replaced by de-ionized water, the well is produced at a low flow rate. Then a fluid conductivity logging probe is run through the wellbore and electric conductivity distribution recorded at several times. Care should be taken not to disturb the wellbore fluid to induce large scale disturbances. With the time sequence of fluid conductivity logs, the inflow characteristics of the fractures can then be determined.

Analytic Considerations

In this section we present a simple analytic method to estimate flowrates q_i and salinity c_i of the fracture fluid. The results will be used later as initial guesses to fit synthetic data.

Given a borehole electric conductivity profiles measured at a given time, such as that given in Figure 2, the area under each peak can be obtained numerically. This can be simply related to qC_o, where q is flow rate in m^3/s and C_o is concentration of the inflow fluid in kg/m^3:

$$\int \sigma(x,t)dx = \alpha(qC_o)\frac{4}{\pi d^2}\cdot t \tag{6}$$

where d is the wellbore diameter, α is coefficient relating salinity with electric conductivity (equation 2) and t is time since the fracture fluid flows into the borehole. This equation assumes that both q and C_o are constant with time. Also the integral on the left-hand-side can only be made at relatively early times before the adjacent peaks overlap significantly as in the case in Figures 3 and 4.

Equation (6) can be applied to a few conductivity profiles, and a plot of $\int \sigma dx$ against t will give as the slope $(4\alpha/\pi d^2)qC_o$ and as the intercept the time, t_o when the fracture fluid starts to flow into the borehole.

In principle, once t_o and qC_o are obtained for each peak, one can apply large-time results, equations (2)-(5), to calculate the flow rate of the particular inflow point. Thus, from careful measurements of early-time log data and late-time log data, one can obtain all the inflow flow rates in a simple and straightforward way. These results are not sensitive to moderate variations of wellbore diffusivity. Note also that while the short-term results depend on wellbore radius, the large-time results are independent of it.

Now if large-time results are not available, as is usually the case in field experiments, we can use the following method to obtain a good first guess of flow rate q from each peak. Figure 6 shows a schematic diagram of a wellbore with several inflow points, each with a flow rate q_i, concentration C_i, and position x_i. The total flow rate out of the well is Q, the initial salinity in the well is C_o, and the inflow at the bottom of the well is W. Positions are indicated assuming the origin at the surface and increasing downward (i.e., depth).

Let L_o be a reference point near the bottom of the well, upstream of (below) the first fracture inflow point, and let L be a point up the well from L_o. At L_o, the conductivity is assumed constant and equal to the initial conductivity k_o. The problem then is to obtain the flow rate Q_L at the point L in the wellbore in terms of the electric conductivity log at different times. Q_L is the sum of all of the q_i's between L_o and L, plus the inflow from the bottom of the well at L_o, W. To simplify the discussion without loss of generality, W will be assumed to be zero in the analysis that follows. Note that taking the difference of two values of Q_L, one upstream of an inflow point and one downstream of the inflow, will yield a value for q_i at that inflow.

If we assume all inflows initiate at the same time (t=0), then the mean concentration, $\bar{C}_L$, in the wellbore over the section between L_o and L is given by the incoming salinity from the inflow points minus the salinity that leaves the section at L with flow rate Q_L:

$$((L_o-L)\pi r^2)\bar{C}_L(t) = ((L_o-L)\pi r^2)C_o + t\sum_{L<\alpha_i<L_o} q_iC_i - Q_L\int_0^t C(L,t)\,dt \qquad (7)$$

where $(L_o-L)\pi r^2$ is the wellbore volume in the section between L_o and L, and C(L,t) is the time-varying salinity at the location L. The first term on the right-hand side represents the background mean salinity in the wellbore.

Now, if the electric conductivity σ is linearly related to salinity, as in equation (2), we can arrive at the following result by simple algebraic manipulations:

$$Q_L = \frac{\alpha t \sum_{L<\alpha_i<L_o} q_iC_i - ((L_o-L)\pi r^2)[\bar{\sigma}_L(t) - \sigma_o]}{\int_0^t (\sigma(L,t)-\sigma_o)\,dt} \qquad (8)$$

where $\bar{\sigma}_L(t)=\alpha\bar{C}_L(t)$ and $\sigma(L,t)=\alpha C(L,t)$. This equation gives the flow rate, Q_L, at any location L in the borehole directly without trial-and-error procedure, and is valid for any time t.

The first term in the numerator of equation (8) is determined as follows. We note that at time t=0, the well is flushed with de-ionized water (or water at constant salinity) with electric conductivity k_o. Then the well is pumped at a constant small flow rate at the wellhead. Thus at each inflow point, an electric conductivity profile will develop. By integrating the areas of the profile at two successive times, t_1 and t_2, near each of these inflow points we can obtain

$$\alpha q_iC_i = \frac{\int_{x_i-\delta_1}^{x_i+\delta_2} \pi r^2(\sigma(x,t_2)-\sigma(x,t_1))\,dx}{t_2 - t_1} \qquad (9)$$

where x_i is the inflow point location and δ_1 and δ_2 are appropriate distances to bracket the local inflow profile. All of the other quantities in the right-hand side of equation (8) can be obtained from the measured electric conductivity profile.

Note that the quantity $(L_o-L)\pi r^2$ is an integral quantity representing the total borehole volume over the section L. Thus equation (8) is not sensitive to local borehole radius variation, a major advantage over the spinner method of measuring flow rates. Because of the integral forms of the terms in equations (8) and (9), the effects of solute dispersion around the peaks within the interval L_o to L do not affect the results. However, dispersion effects at or near L introduce an error in the value of C(L,t) or k(L,t). This, we believe, is a source of uncertainty in our parameter estimation. Examining the values of Q_L determined from equation (8) at a series of locations between two successive peaks illustrates this uncertainty. At these locations, we know that Q_L should be constant. The variation in Q_L is a measure of solute dispersion in the borehole and can probably be studied to cancel its effect and obtain the proper values of the flow rate. An alternative is to solve for Q_L using equation (8) and then slightly adjust the value to match the data using the code BORE. In this paper, the latter approach is used.

If q_iC_i is constant for all inflow points, equation (8) holds for any time t. Thus we can solve the problem at a few different time periods and the result should be the same. This is a good internal check. This also means that short term data may be sufficient to give accurate results. A reduction of the necessary measurement time (say, from 600 hours to 100 hours) represents a major savings in testing cost, and makes the technology more commercially applicable.

On the other hand, if any q_iC_i changes with time, Q_L will also change with time. Thus applying equation (8) at different times will tell us (probably crudely) how q_i changes with time. Note that if C_i changes with time, but not q_i, we expect Q_L obtained by equation (8) will be the same at different times (so long as t_2 is set equal to t and t_1 equal to 0 in equation (9)). This means that the equation is applicable even when C_i from each inflow point is time varying!

Now, in field operations, because of the fluid logging procedure or changing flow rates (transient effects), it is conceivable that the fluid flows from the fractures into the wellbore do not initiate at the same time, but at t_{α_i} respectively, then an estimate for t_{α_i} is obtained as follows:

$$t_{\alpha_i} = t_1 - \frac{\int_{x_i-\delta_1}^{x_i+\delta_2} \pi r^2(\sigma(x,t_1)-\sigma_o)\,dx}{\alpha q_iC_i} \qquad (10)$$

And equation (8) can also be easily modified to take this into account:

$$Q_L = \frac{\alpha \sum_{L<\alpha_i<L_o} (t-t_{\alpha_i})q_i C_i H(t-t_{\alpha_i}) - ((L_o-L)\pi r^2)[\bar{\sigma}_L(t)-\sigma_o]}{\int_{t_L}^{t} (\sigma(L,t)-\sigma_o)\,dt} \tag{11}$$

where $H(t-t_{\alpha_i})$ is the Heaviside step function, which is 1 for $t>t_{\alpha_i}$ and 0 for $t\le t_{\alpha_i}$. Here in the denominator the lower limit of integration, t_L, is taken as the time at which $k(L,t_L)$ at L begins to be greater than the background concentration value k_o.

Now $(t-t_{\alpha_i})q_i C_i$ represents the total salinity input into the borehole. If, at time t after the initial washing out of the borehole with de-ionized water, the conductivity log is measured, we can set $t_1=0$ and $t_2=t$ in equation (9), the total salinity input into the borehole is:

$$\frac{1}{\alpha}\int_{x_i-\delta_1}^{x_i+\delta_2} \pi r^2 (k(x,t)-k_o)\,dx \tag{12}$$

regardless of the values of t_{α_i} and also regardless of whether q_i or C_i is time dependent or not. Then equation (11) can be generalized to:

$$Q_L = \frac{\sum_{L<\alpha_i<L_o} \int_{x_i-\delta_1}^{x_i+\delta_2} \pi r^2 (k(x,t)-k_o)\,dx - ((L_o-L)\pi r^2)[\bar{k}_L(t)-k_o]}{\int_{t_L}^{t} (k(L,t)-k_o)\,dt} \tag{13}$$

Here Q_L has to be interpreted as a type of mean flow rate over the time period 0 to t, at location L. So far we have applied equations (8) and (9) to problems presented in Section 4 below. We are in the process of testing the use of equations (12) and (13) for time-varying q_i and C_i.

The equation (8) assumes all solute flux is flowing up the wellbore and thus does not apply to locations in the wellbore where the solute flux is mainly down the borehole by diffusion. This is not a major restriction because avoiding these locations does not prevent us from obtaining the flow profile in the wellbore. In principle, all we need is to apply the equation to a point at the downstream side (up the borehole) of each inflow point.

A special case is when L is small and is below (or upstream of) the first inflow point. If we apply equation (8) in this case, we obtain the indeterminate result of $Q_L=0/0$. This is not surprising, indicating the simple result that without input salinity, it is not possible to determine the flow rate.

Numerical Method

For a general problem of multiple inflow points, overlapping salinity curves and variable dispersion coefficient K, no analytic solution is readily available and numerical methods are required. For our purpose, we developed a simple computer code (Hale and Tsang, 1988) that solves the linear advective-dispersive equation:

$$K\frac{\partial^2 C}{\partial x^2} - v\frac{\partial C}{\partial x} + S = \frac{\partial C}{\partial t} \tag{14}$$

where C is the concentration of solute, K is the dispersion coefficient, v is the linear borehole fluid velocity, and S is the source term, under the initial condition:

$$C(x,0) = C_o(x) \qquad x \le x_{max},\ t=0\,. \tag{15}$$

Here x_{max} represents the deepest point of interest in the borehole. The code uses a finite difference solution scheme with upstream weighting and can accommodate various boundary conditions. It has been verified against a number of analytic solutions and also against a well-validated numerical code, PT (Bodvarsson, 1982; Tsang 1985; Tsang and Doughty, 1985).

Figure 7 shows the numerical results of a case with one inflow point under an overall inflow flow rate w. Figure 8 shows a late-time numerical solution for the case of the overall wellbore fluid flow rate w equal to 0, q/3 or q, where q is the fracture inflow rate. The saturation salinity values are C_o, 3/4 C_o and 1/2 C_o

respectively. This is obvious from the proportionate mixing of inflow salinity with the upcoming wellbore flow with $C_w = 0$ (equation 3). Note that we are using the volume flow rates w and q and not linear velocities. Thus, the variation of wellbore cross-section has no effect on these results.

Figure 9 shows the salinity curves in the wellbore w = 0. Because there is a closed boundary at well bottom x = 0, there is still a preferred flow upwards to -x values. This can be seen easily if the closed boundary is represented by image sources below it. With inflow at rate q at the point x = -50 m, the flow rate in the wellbore is q downstream from x = -50 m and 0 upstream.

Figure 10 shows the interference between two inflow points. In all of these cases K is taken to be 1.25×10^{-5} m^2/s and the overall wellbore flow rate to be $w = 1.5 \times 10^{-7}$ m^3/s. The two inflow points are at x = -50 m and x = -100 m with flow rates q_1 = and $q_2 = 3 \times 10^{-7}$ m^3/s. Interference effects are seen as a sudden jump in the curve when the salinity curve from the upstream inflow point overlaps the downstream point. Figure 10 also shows the large time period results with a step structure at large times confirming that shown in Figure 4.

A synthetic data set composed of a time-series of conductivity logs with times ranging from 0.5 to 600 hours was generated by the code BORE. Four inflow points were used. The synthetic logs for 0.5, 144 and 600 hours are shown in Figure 11. The data set is designed so that they are realistic, similar to the real field data obtained from the Leuggern hole in Switzerland.

PRE was used to estimate the inflow parameters using various subsets of the time-series of logs, with successively larger final times (i.e. using the first five logs, the first eight, the first ten, etc.). The resulting estimates of the parameters, shown in Table 1, indicate that the values stabilize at relatively short times (less than 100 hours), and that the use of additional logs provides little additional information. This may mean that the test need only be carried out for 100 hours. This is due to the fact that the values of q_iC_i are based on early times, and the data at later times only enter into the integral in the denominator of the equation for Q_L.

The predicted profile of conductivity logs based on parameters obtained by applying PRE to the 96 hour data is shown in Figure 12. The agreement with the synthetic data is already very good, with the exception of the inflow at 915m. Minor adjustments result in a good fit to the synthetic data, as shown in Figure 13.

Conclusion and Discussion

In this paper we first discussed the procedure and physical processes associated with a time series of fluid conductivity logs in a borehole intersected by a number of flowing fractures. Simple formulas to evaluate some of the relevant parameters are described and their uses demonstrated. Then numerical matching of the data to obtain the remaining parameters is shown. The results are not sensitive to borehole radius variations and the method may be able to measure small inflow rates.

Acknowledgements

Discussions and cooperation with NAGRA personnel, especially P. Hufschmied, M. Thury, A. Zingg, and P. Zuidema are much appreciated. Assistance in computation and graphing from C. Doughty is gratefully acknowledged. We would also like to thank C. Doughty, N. Goldstein, and I. Javandel for reviewing and commenting on the manuscript. This work is jointly supported by the Director, Office of Energy Research, Office of Basic Energy Sciences, Engineering and Geosciences Division, and the Director, Office of Civilian Radioactive Waste Management, Repository Technology and Transport Program (DOE/CH) of the U. S. Department of Energy through Contract No. DE-AC03-76SF00098.

References

Bean, H. S. (1971), *Fluid meters: Their theory and application*, American Association of Mechanical Engineers, 6th Edition, New York.

Bodvarsson, G. S. (1982), Mathematical modeling of the behavior of geothermal systems under exploitation, Ph.D. Thesis, University of California at Berkeley, Department of Materials Sciences and Mineral Engineering.

Hale, F. V. and C. F. Tsang (1988). A code to compute borehole fluid conductivity profiles with multiple feed points, LBL-24928, Lawrence Berkeley Laboratory, Berkeley, CA.

Hufschmied, P. (1983), Ermittlung der Durchlässigkeit von Lockergesteins - Grundwasserleitern, eine vergleichende Untersuchung verschiedener Feldmethoden, Diss. No. 7397, ETH Zurich, Switzerland.

Hess, A. E. (1985), Identifying hydraulically-conductive fractures with a low velocity borehole flowmeter, *Canadian Geotech. Journal*, *23* (1), 69-78.

Omega (1987), *Complete Flow and Level Measurement Handbook and Encyclopedia*. Omega Engineering, Inc., Stamford, Connecticut.

Paillet, F. L., Hess, A. E., Cheng, C. H. and Hardin, E., (1987), Characterization of fracture permeability with high resolution vertical flow measurements during borehole pumping, *Ground Water*, *25* (1) 28-40.

Shedlovsky, T., and L. Shedlovsky (1971), "Conductometry," *Techniques of Chemistry*, (Arnold Weissberger and Bryant W. Rossiter, eds.), Vol. 1. Physical Methods of Chemistry, Part IIa, Electrochemical Methods, John Wiley & Sons, Inc., New York.

Tsang, C. F. (1985), Lessons learned in the verification and validation studies of a coupled heat and fluid flow code, Invited Paper, Proceedings of Symposium on Groundwater Flow and Transport Modeling for Performance Assessment of Deep Geologic Disposal of Radioactive Waste: A Critical Evaluation of the State of the Art, May 20-21, 1985, Albuquerque, New Mexico.

Tsang, C. F. and C. Doughty (1985), Detailed validation of a liquid and heat flow code against field performance, Proceedings of the Eighth SPE Symposium on Reservoir Simulation, February 10-13, 1985, Dallas, Texas, organized by Society of Petroleum Engineers, Richardson, Texas.

Table 1. Parameter Estimates for Synthetic Case

Time of Latest Log (hrs)	Inflow Rate (l/min)			
	q_{850}	q_{915}	q_{1200}	q_{1440}
8	3.4	0.53	0.29	0.11
12	4.7	0.55	0.30	0.12
24	4.8	0.58	0.30	0.11
48	5.0	0.65	0.32	0.10
96	4.9	0.60	0.32	0.093
144	4.9	0.59	0.30	0.088
288	4.9	0.58	0.33	0.083
600	4.9	0.58	0.30	0.081
Fit by slight adjustments from 96	4.8	0.23	0.24	0.066
Input	4.3	0.27	0.22	0.070

Time of Latest Log (hrs)	Inflow Concentration (kg/m^3)			
	C_{850}	C_{915}	C_{1200}	C_{1440}
8	1.0	1.6	0.52	0.46
12	0.77	1.5	0.50	0.42
24	0.75	1.4	0.49	0.45
48	0.72	1.3	0.47	0.49
96	0.73	1.4	0.47	0.54
144	0.73	1.4	0.50	0.57
288	0.74	1.4	0.46	0.60
600	0.74	1.4	0.50	0.61
Fit by slight adjustments from 96	0.85	3.1	0.68	0.72
Input	0.85	3.1	0.68	0.71

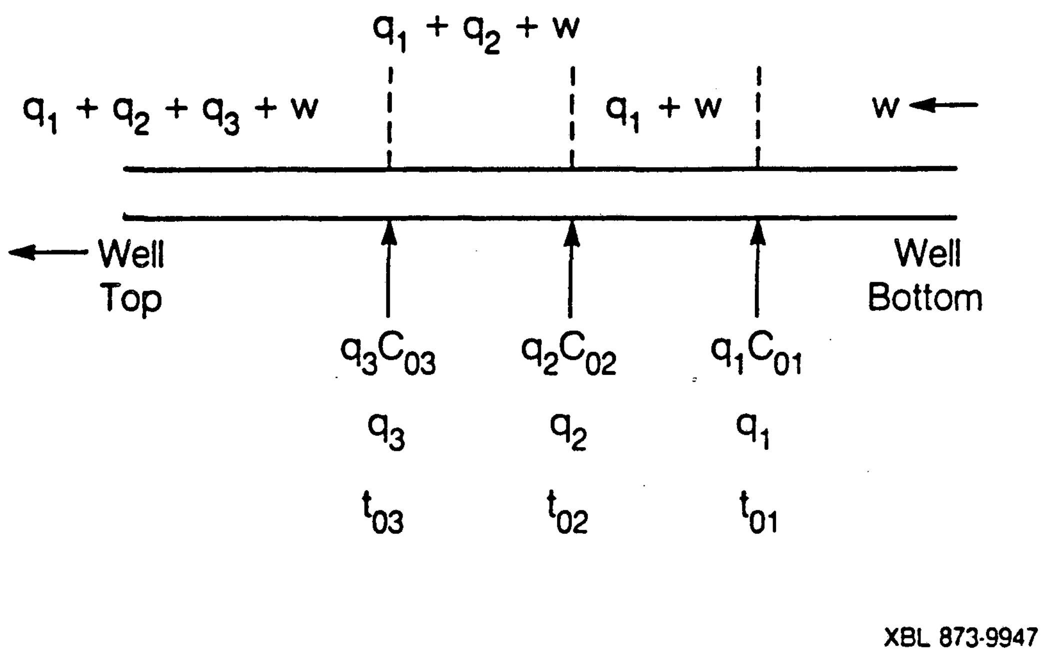

Figure 1. Schematic picture of a wellbore with three inflow points and a well-bore flow rate w from below.

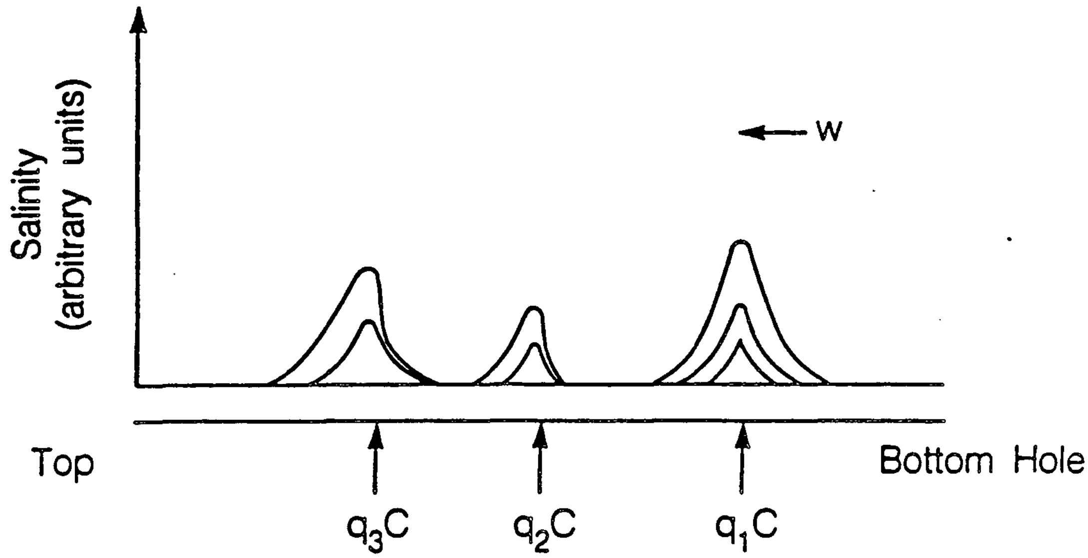

Figure 2. Schematic picture of salinity curves from three inflow points in a wellbore at early times.

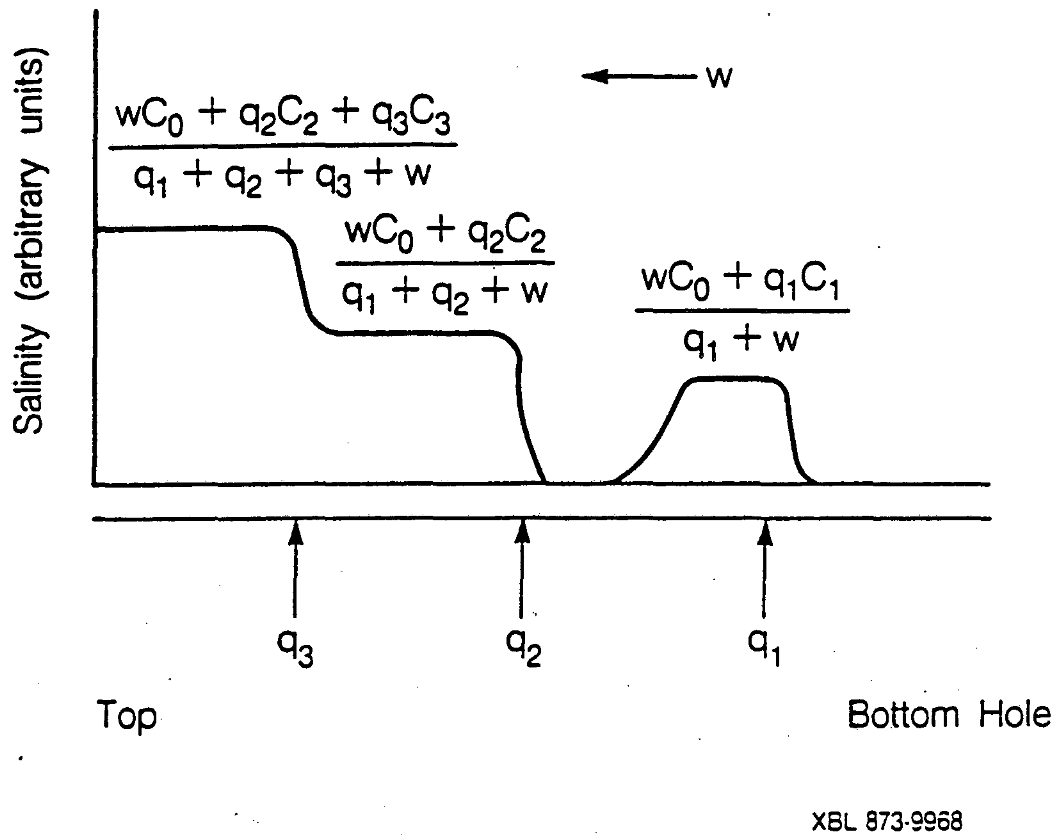

Figure 3. Schematic picture of salinity curves at a large time, assuming very small diffusion effects.

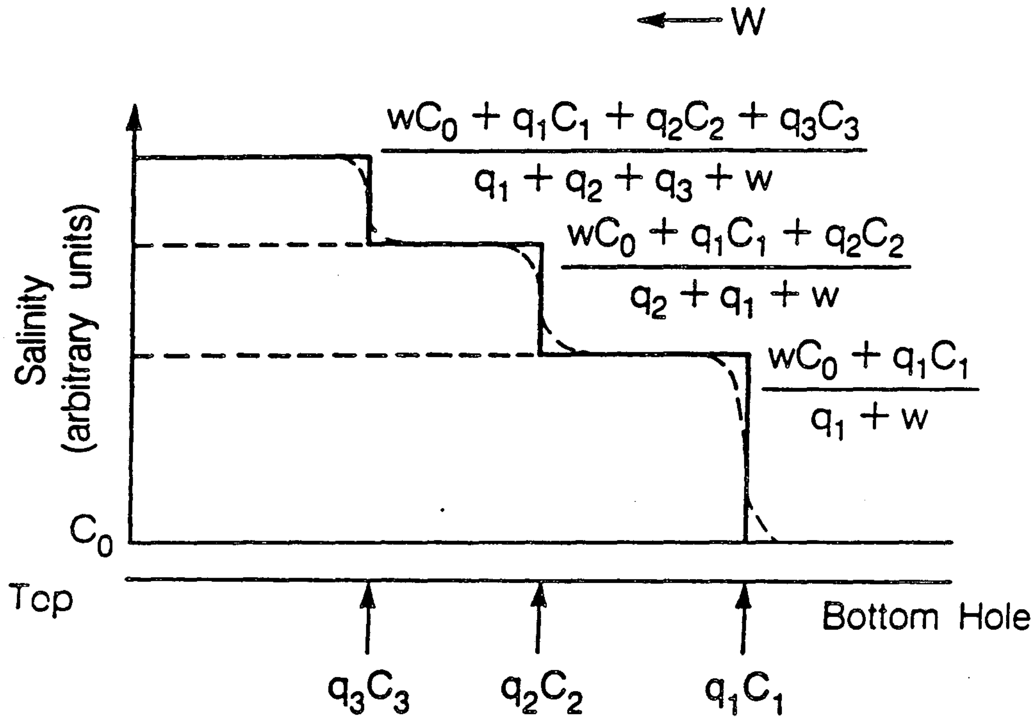

Figure 4. Schematic picture of salinity concentration curves at the very large time limit, assuming very small diffusivity effects.

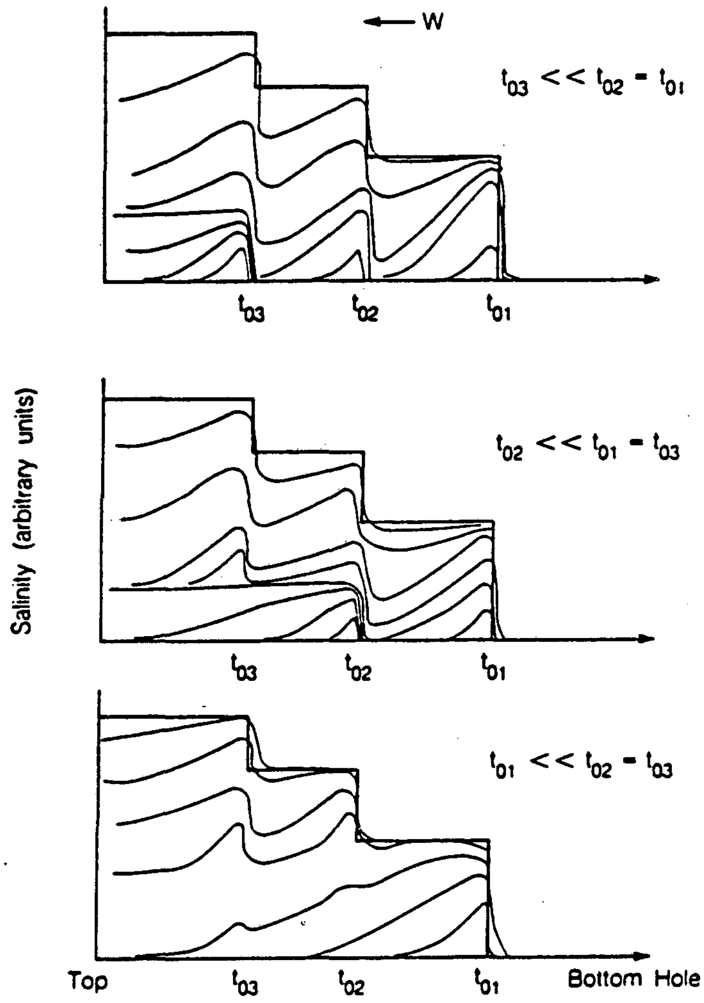

XBL 873 9946

Figure 5. Schematic picture of salinity concentration curves from early to later times, assuming one of the three inflow points begins much earlier than the other two.

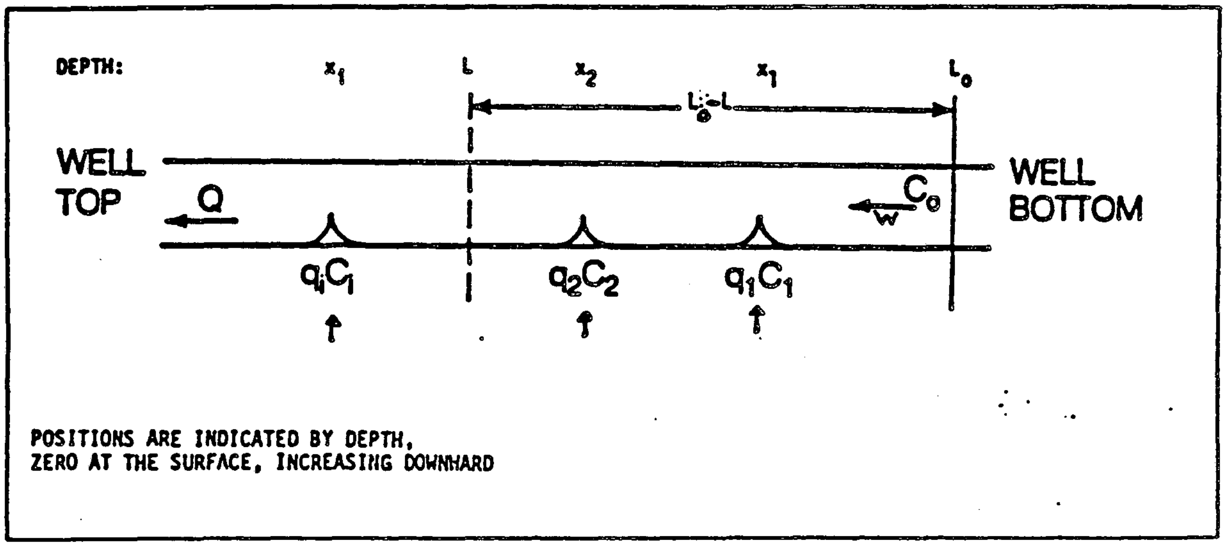

Figure 6. Schematic diagram of a wellbore with several inflow points, each with a flow rate Q_i, concentration C_i, and position x_i. The total flow rate out of the well is Q, the initial salinity is C_0, and the inflow at the bottom of the well is W. Positions are indicated assuming the origin at the surface and increasing downward (i.e., depth).

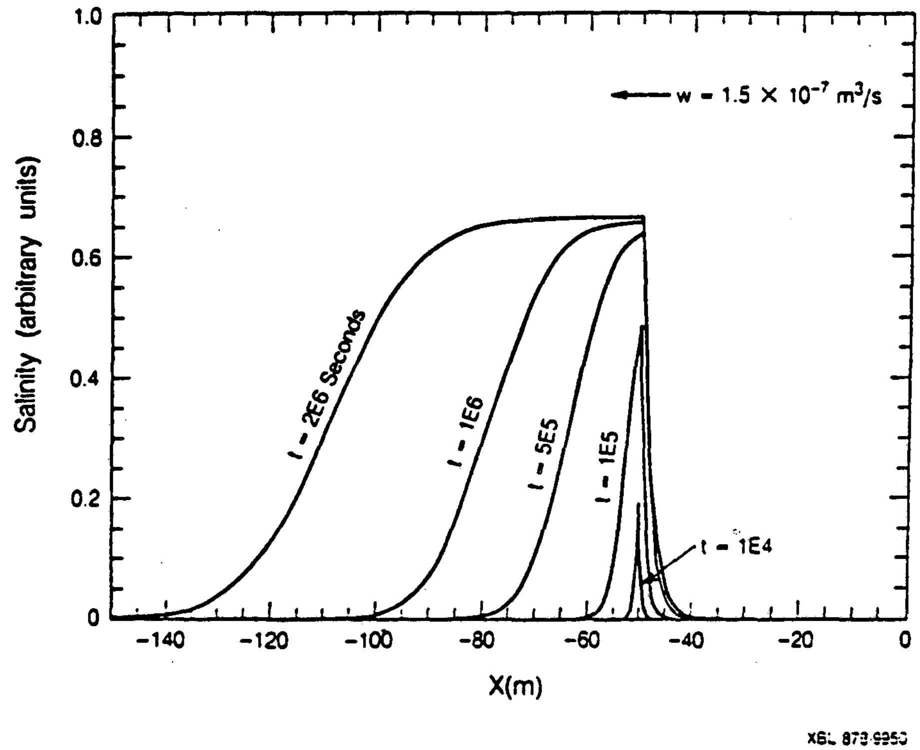

Figure 7. Numerical results for one inflow point from early to later times.

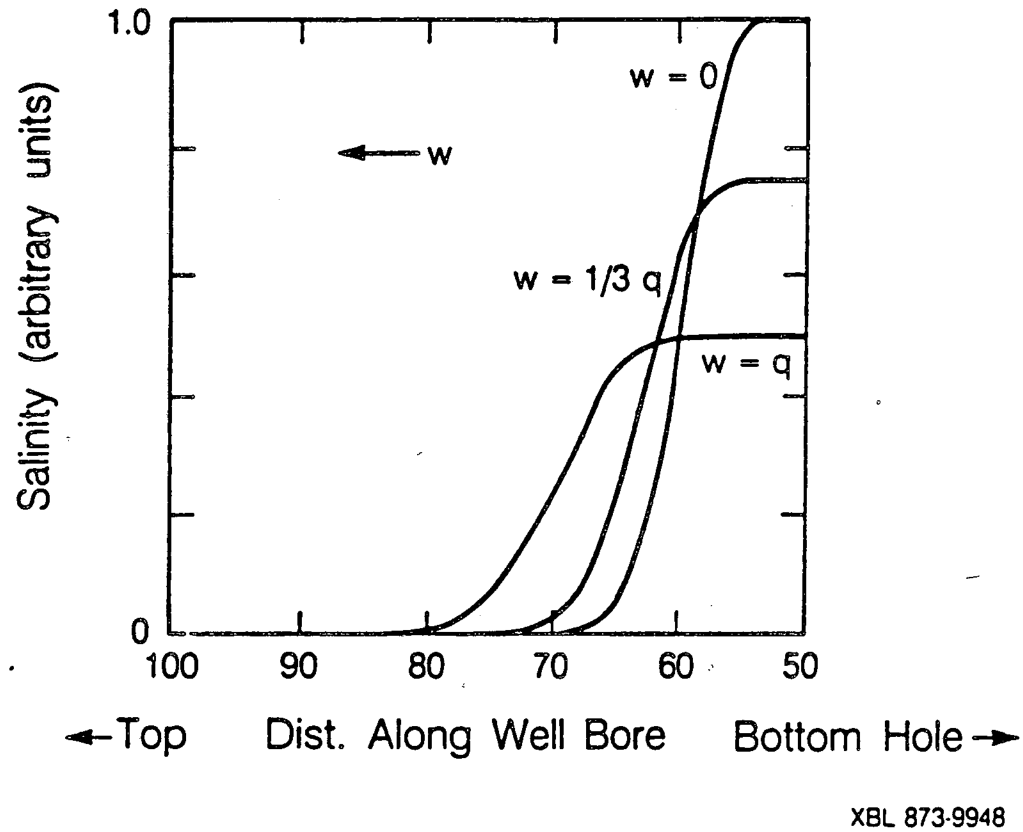

Figure 8. Numerical results for one inflow point at flowrate q for three values of wellbore flow rate from below: $w = 0$, $w = q/3$ and $w = q$.

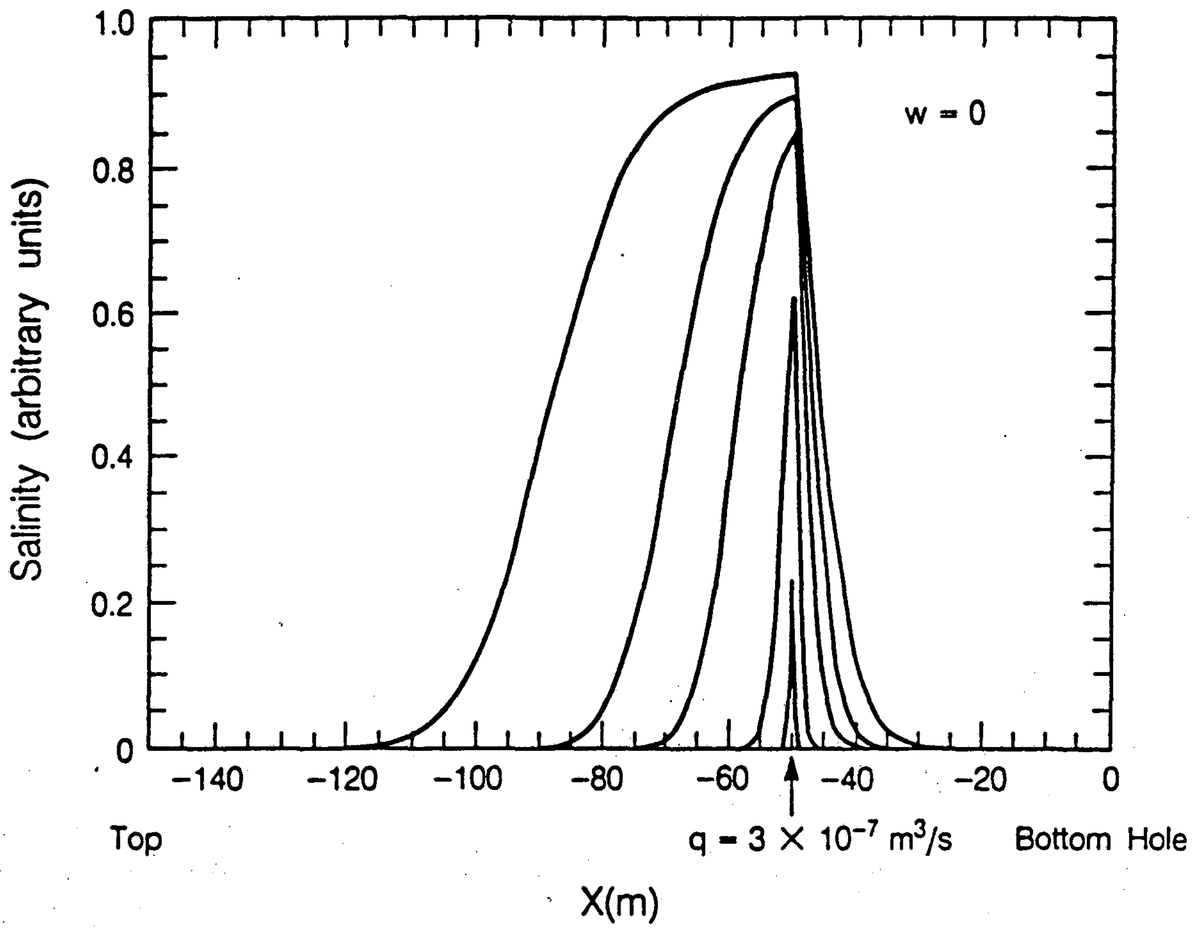

Figure 9. Numerical results for one inflow point and w = 0 for dispersion constant K equal to 50 m^2/s.

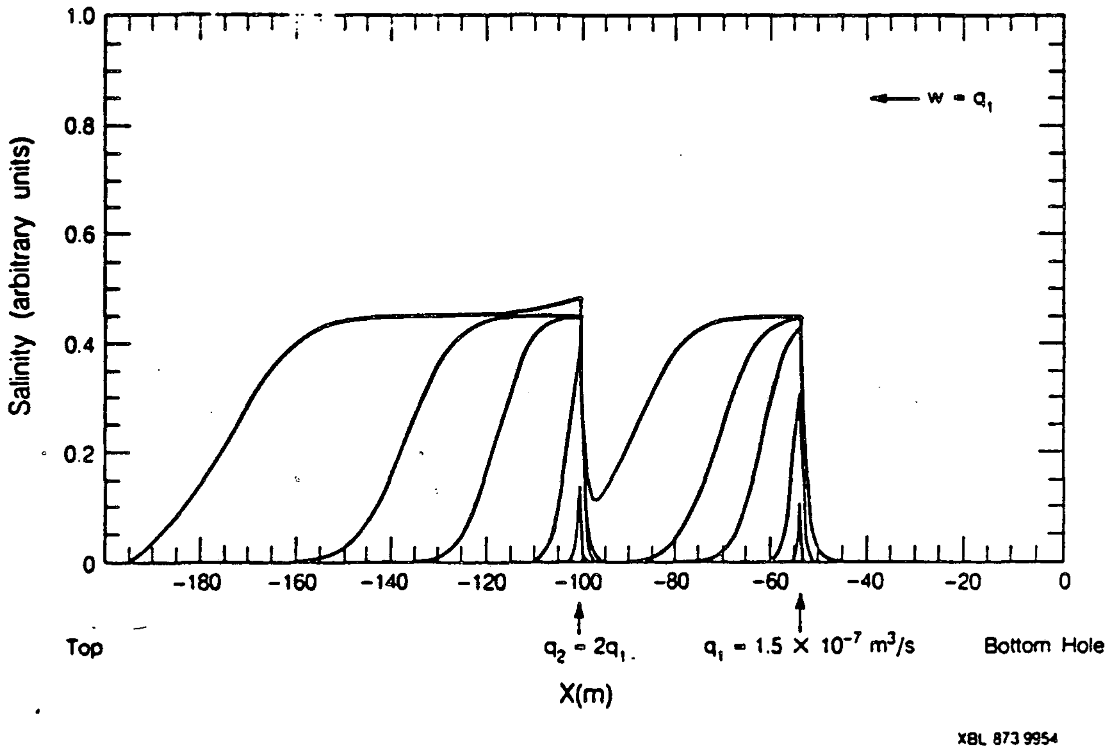

Figure 10. Numerical results for two inflow points.

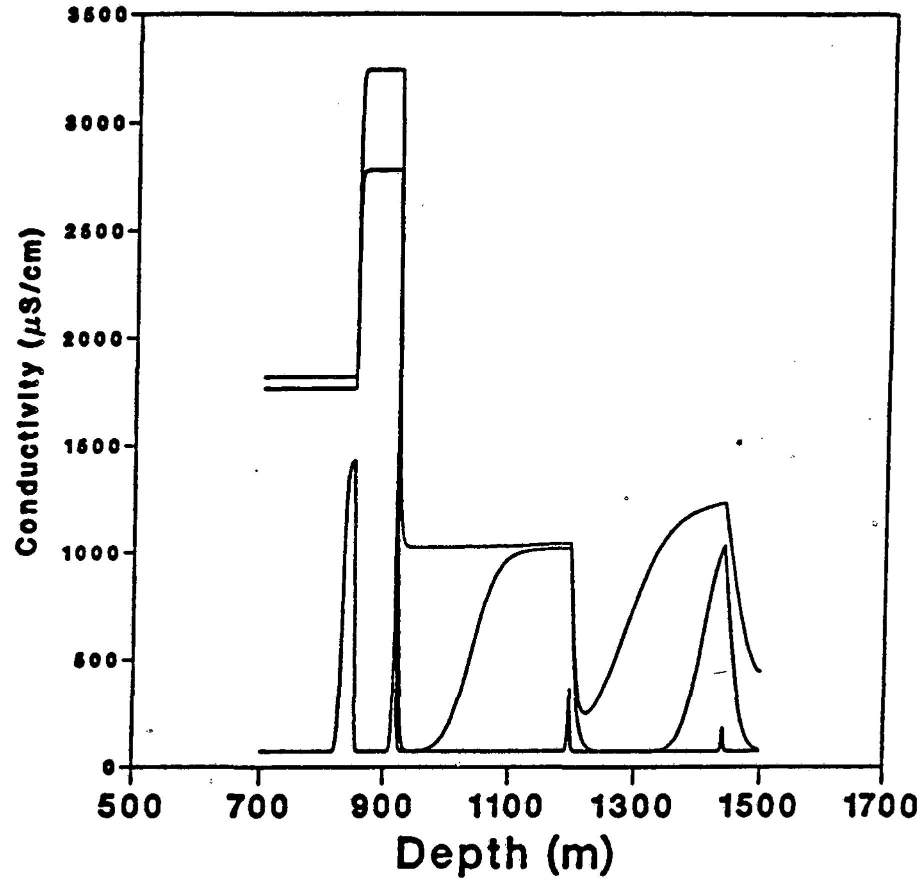

Figure 11. Schematic at 0.5, 144 and 600 hrs.

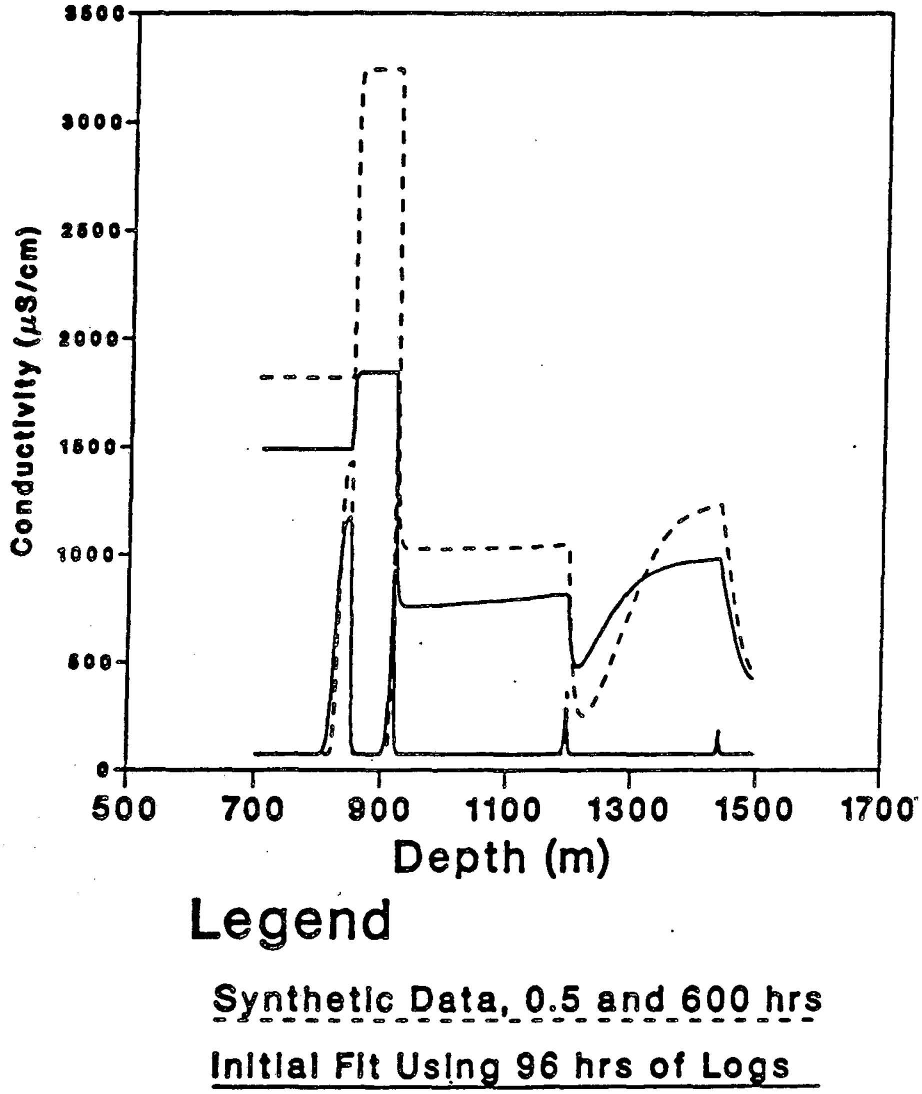

Figure 12. Synthetic initial estimate.

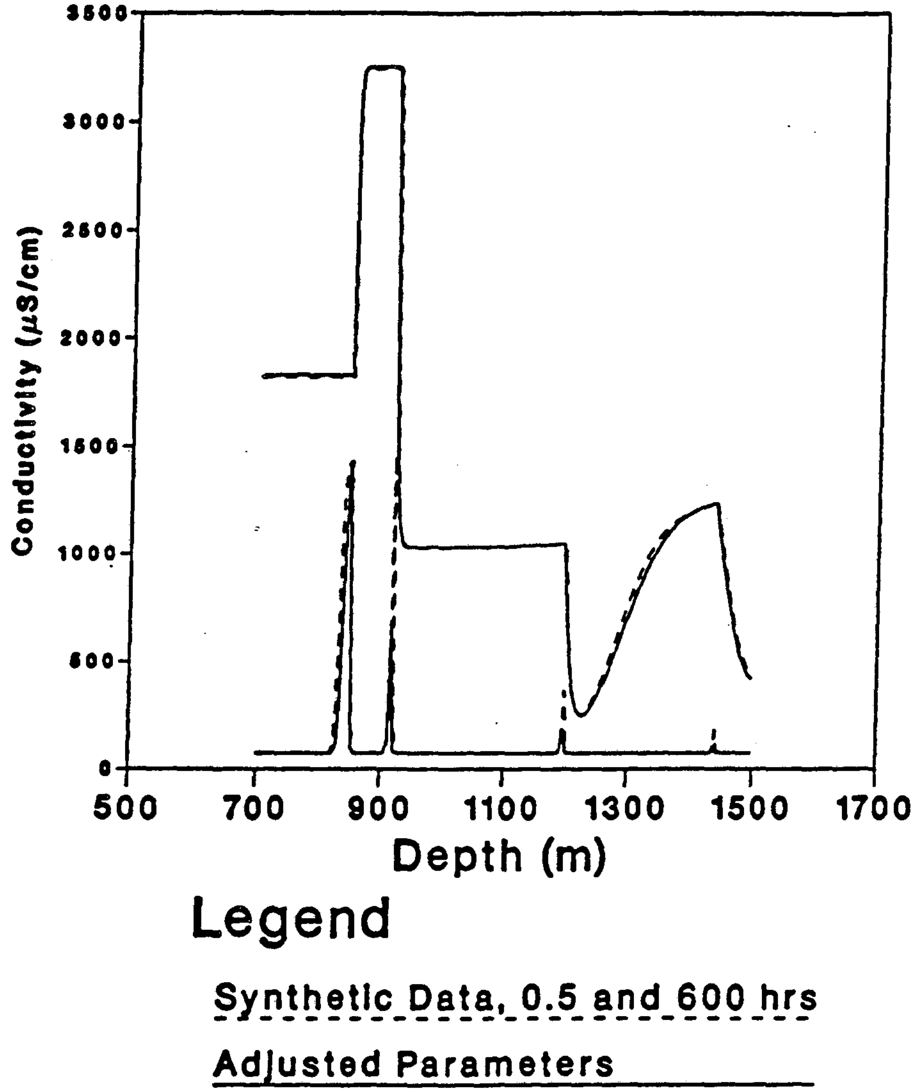

Figure 13. Adjust parameters.

LAWRENCE BERKELEY LABORATORY
TECHNICAL INFORMATION DEPARTMENT
1 CYCLOTRON ROAD
BERKELEY, CALIFORNIA 94720